SLAC – PUB – 4386
August 1987
(E)

EXPERIMENTAL STUDIES OF ELECTROMAGNETIC PROPERTIES OF FEW BODY SYSTEMS*

P. E. Bosted

The American University, Washington D.C. 20016
and
Stanford Linear Accelerator Center, Stanford, CA 94305

ABSTRACT

An overview is given of some recent and planned experiments which have or will substantially increase our knowledge of the electromagnetic properties of the few body systems. Specific examples include the proton and neutron elastic form factors, the deuteron elastic form factors, deuteron threshold electrodisintigration and quasi-elastic scattering, deuteron photodisintigration, and finally measurements of R in deep inelastic scattering from hydrogen, deuterium, and iron.

INTRODUCTION

The availability of a large current, medium energy electron beams at institutions such as SLAC, Bates, and Saclay has been combined with improvements in detectors and experimental techniques to push our knowledge of the electromagnetic properties of the few body systems to ever higher momentum transfer Q^2 and ever greater accuracy. The topic is too vast to cover completely in a paper such as this, so that I will concentrate on a few areas where recent or planned experiments are making significant contributions. See Ref. 1 for reviews that cover additional topics such as elastic and inelastic scattering from the tri-nucleon systems.

PROTON ELASTIC FORM FACTORS

Probably the simplest few body system of interest to nuclear physicists is the nucleon. In most cases the properties of nuclei can be explained in terms of systems of bound nucleons, ignoring the internal structure of the nucleons. Recent experimental evidence, especially the 'EMC Effect', has shown that at high energies this assumption breaks down. A central question has become to what extent are nucleon properties changed when in a nucleus, and what is the probability that two nucleons form a dibaryon state when placed close together. Answers to these and other questions require the best possible knowledge of the free nucleon properties and the development of good theoretical frameworks for explaining them.

* Work supported in part by the Department of Energy, contract DE-AC03-76SF00515 (SLAC) and by the National Science Foundation, Grant PHY85-10549 (American University).

Invited talk presented at the CEBAF Summer Workshop
Newport News, Virginia, June 22-26, 1987

Measurements of the nucleon form factors are usually given in terms of the Sachs form factors

$$G_E = F_1 - \frac{Q^2}{4M^2} F_2 \tag{1}$$

$$G_M = F_1 + F_2 \tag{2}$$

where F_1 and F_2 are the Dirac and Pauli form factors, which give information on the charge and spin distributions respectively. At low energies, a successful phenomenological description of the form factors can be given in terms of vector dominance models[2] (VDM) in which the interaction is pictured to be composed of two parts: a bare photon and vector meson components to the photon. At sufficiently high energy the role of vector mesons is expected to diminish, and calculations of the hard photon scattering should be possible using perturbative QCD. A major question has been how high does the energy transfer have to be for PQCD to work?

Recent experimental data[3] has shed some light on this question. Electrons with energies up to 20 GeV were scattered from a 60 cm long hydrogen target in End Station A at SLAC. The use of longer target, more forward angle, better detectors in the spectrometer, and the masking of the target endcaps were the principal factors that permitted measurements from $Q^2 = 2.9$ to 31.3 $(\mathrm{GeV/c})^2$ with considerably smaller errors than previous measurements. The results for the quantity $Q^4 G_M^p/\mu_p$ are shown in Figure 1, extracted from the measured cross sections assuming that $G_E^p = G_M^p/\mu_p$. The results show $Q^4 G_M^p$ attaining an approximately constant value around 5 to 10 $(\mathrm{GeV/c})^2$. This is consistent with the PQCD prediction[4] that F_1 should fall as Q^{-4} (times a slowly falling function of Q^2 due to the running of the strong coupling constant α_s and terms proportional to $\ln(Q^2)$), while F_2 should fall as Q^{-6} due to the extra helicity flip. Explicit calculations have so far been done for F_1 only. The results have been found to be quite sensitive to the choice of quark wave function. A symmetric wave function gives a curve[4] with the right shape (solid curve normalized to the

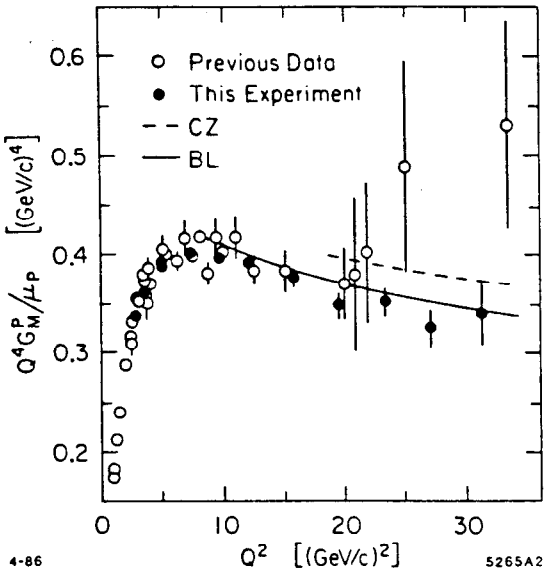

Fig. 1. New results for the proton form factor G_M^p from Ref. 3. The perturbative QCD curves are from Ref. 4 (BL) and Ref. 5 (CZ).

data at $Q^2 = 10$ (GeV/c)^2) but a magnitude that is about a hundred times too small. Chernyak and Zhitnitsky[5] have derived a set of asymmetric wave functions which satisfy the constraints from QCD sum rules and also give good agreement with the size and shape for G_M^p (dashed curve in Fig. 1).

Several developments should take place before one could conclude that PQCD becomes applicable around $Q^2 = 5$ (GeV/c)^2 and that the valence quarks in the nucleon do not share momentum equally. The first is that numerical calculations of F_2 are required. It is quite possible that the slow decrease in $Q^4 G_M^p$ with Q^2 is not due to the running of α_s and the $\ln(Q^2)$ terms, but to there being a substantial contribution to G_M^p from F_2 in this Q^2 range. This can be seen in an extended VDM fit (which required that $F_1 \sim C_1/Q^4$ and $F_2 \sim C_2/Q^6$ at high Q^2) made by Gari and Krumpelmann[6] (see Figure 2). On the experimental side, measurements of G_E^p are sorely needed. For example, if $G_E^p = G_M^p$ above $Q^2 = 6$ (GeV/c)^2, rather than $G_E^p = G_M^p/\mu_p$, as suggested by one diquark model,[7] than the values for $Q^4 G_M^p$ extracted from the measured cross sections would be almost completely independent of Q^2 above $Q^2 = 6$ (GeV/c)^2, instead of showing the slow decrease seen in Figure 1.

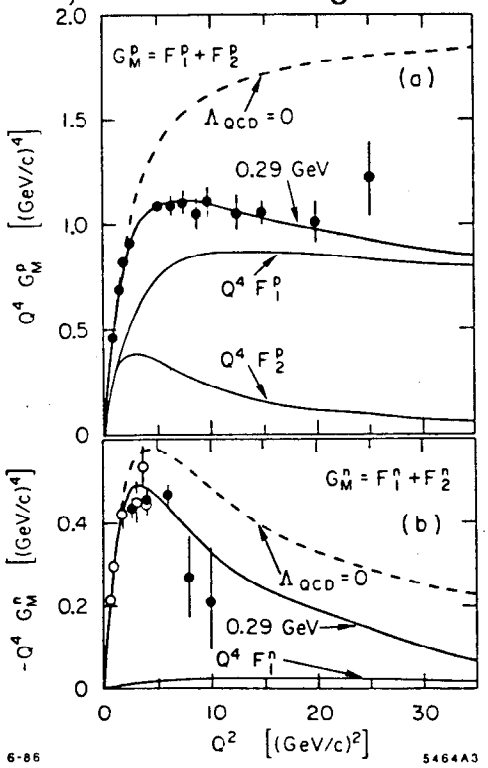

Fig. 2. Data for a) G_M^p and b) G_M^n compared to VDM + QCD fit of Ref. 6.

Aside from their value in interpreting the high Q^2 SLAC data, measurements of G_E^p are interesting in their own right in providing additional constraints on the VDM fits and probing the transition region to PQCD. The existing data (divided by the dipole law $G_D = 1/(1 + Q^2/.71)^2$) are shown in Figure 3, along with some of the VDM models. The error bars do not permit discrimination among models above $Q^2 = 3$ (GeV/c)^2. Not shown are preliminary results from a recent Rosenbluth experiment[8] at SLAC which made measurements up to $Q^2 = 3$ (GeV/c)^2. The new data do not show any significant deviation from the dipole law. Further measurements[9] at SLAC using the Rosenbluth separation method are planned up to approximately $Q^2 = 6$ (GeV/c)^2 with an error on G_E^p/G_D of ± 0.15 at the highest Q^2 (open rectangles in Figure 3). To achieve these small errors requires measurements over a large range of the polarization parameter ϵ. Forward angle measurements are needed with beam energies of 10 GeV or more, while backward angle measurements require a spectrometer

with a large solid angle to maintain reasonable count rates. Very good control over systematic errors is also required. Due to its limited beam energy, CEBAF will probably not be able to go much higher in Q^2 using the Rosenbluth method, but could likely obtain significantly smaller errors at moderate Q^2 by using combinations of polarized beams, polarized targets, and polarimeters to measure assymetries which are directly proportional to G_E^p.

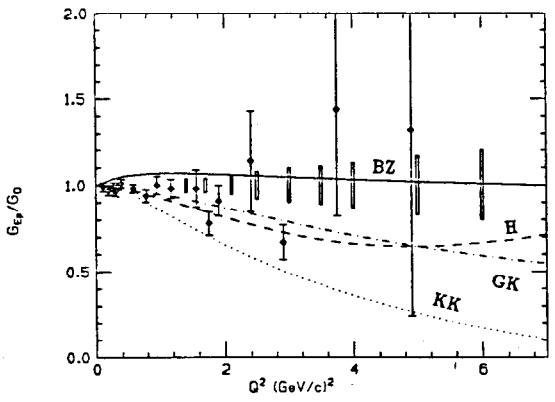

Fig. 3. Existing data for G_E^p compared to some VDM fits.[2] The open rectangles show the expected errors from a future SLAC experiment.[9]

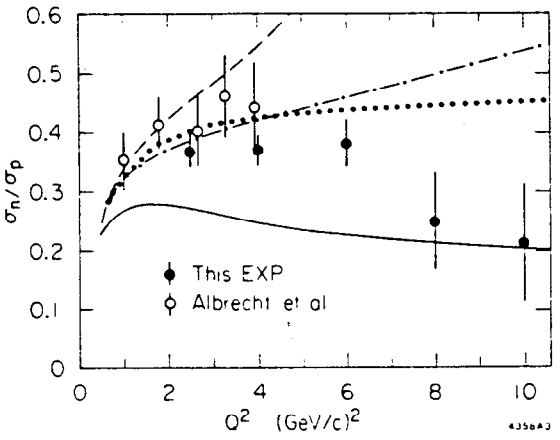

Fig. 4. Data[10] for σ_n/σ_p compared to VDM models of Höhler et al.[2] (dashed) and Blatnik and Zovdko[2] (solid) and to form factor scaling (dotted) and the dipole law (dashed-dot).

NEUTRON ELASTIC FORM FACTORS

Experimental knowledge of the neutron form factors has been necessarily much more limited than that of the proton due to the lack of a free neutron target. Most experiments have been performed using the deuteron as a target and subtracting the contribution from the proton. Existing measurements[10] of the ratio of neutron to proton cross sections at forward angles are shown in Figure 4. The results were all obtained from quasi-elastic scattering from the deuteron, and the error bars are dominated by the uncertainty in subtracting inelastic contributions rather than by statistics. The data show a fairly constant ratio between $Q^2 = 1$ and 6 (GeV/c)^2, then a slow decrease at high Q^2. The agreement with older VDM fits (done before the neutron data was available) is not particularly good, nor do the high Q^2 data seen to be in good agreement with empirical relations such as form factor scaling ($G_M^p/\mu_p = G_E^p = G_M^n/\mu_n$ and $G_E^n = 0$) or the dipole law ($G_M^n/\mu_n = G_D$ and $G_E^n = 0$). The best description of the data comes from models[6,11] in which F_1^n is small compared to F_2^n (see Figure 2). Calculations in PQCD have yet to be performed, but would likely shed light on the origin of the differences between proton and neutron cross sections.

The separation of the electron and magnetic form factors of the neutron has proven to be extremely difficult experimentally. The existing data for $(G_E^n/G_D)^2$ (see Figure 5) show that G_E^n is much smaller than G_M^n at low Q^2, and are equally compatible with either $F_1^n = 0$ or $G_E^n = 0$. The experiment[9] approved to run at SLAC to extend the measurements of G_E^p to high Q^2 will also try to extend the separation of G_M^n and G_E^n to $Q^2 = 4$ (GeV/c)^2 by performing Rosenbluth separations on quasi-elastic scattering from deuterium. The anticipated error bars from this experiment are shown as the tall rectangles in Figure 5 and should be small enough to distinguish between $F_1^n = 0$ and $G_E^n = 0$. While much of the relatively large errors come from counting statistics and the need to subtract the effect of the proton, a detailed knowledge of how the cross section deviates from the impulse approximation will be needed to have full confidence in the results. The error bars shown include estimates for all these possible sources of uncertainty. Plans also exist to make precision measurements of G_E^n at Bates at relatively low Q^2 using both polarization transfer (polarized beam and neutron polarimeter) and the scattering of polarized electrons from a polarized ^3He target. These measurements could be extended to higher Q^2 at CEBAF.

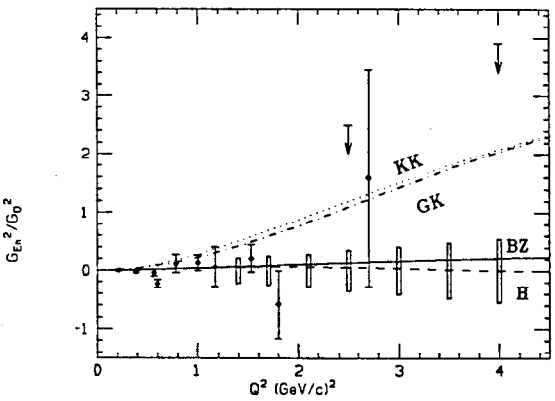

Fig. 5. Existing (solid circles) and potential (open rect.) data for $(G_E^n/G_D)^2$. Curves GK[6] and KK[11] have $F_1^n = 0$.

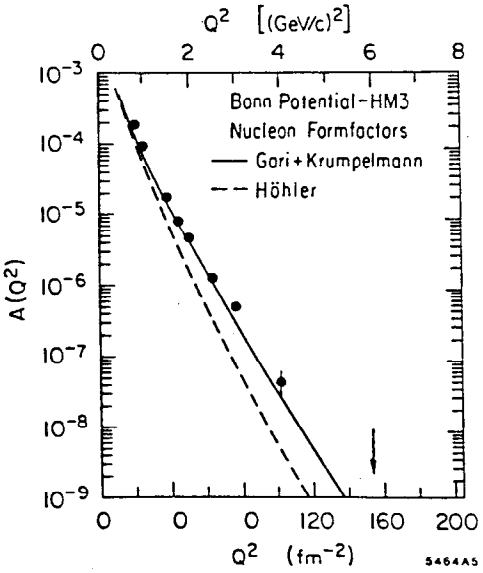

Fig. 6. Data for deuteron $A(Q^2)$ compared to IA calculations[12] with nucleon form factors from Refs. 2 and 6.

A better knowledge of the nucleon form factors will be important in interpreting existing and potential data from nuclear targets. A first example is the forward angle form factor of the deuteron $A(Q^2)$. As shown in Figure 6, the choice of form factors can change the calculations by a factor of 4 at $Q^2 = 4$ (GeV/c)^2. Another example is in quasi-elastic scattering from nuclei, where the longitudinal strength has been found to be smaller than expected.[13]

The choice of form factors can change[14] the predicted longitudinal strength at $Q^2 = 1$ (GeV/c)^2 by 25% for most nuclei and as much as 40% for ^3H. The effect is even larger at higher Q^2. It is vital to know the nucleon form factors before one can blame the disagreement between calculations and data for the longitudinal response function on more exotic effects.

DEUTERON ELASTIC FORM FACTORS

The electromagnetic form factors of the deuteron at high momentum transfer have long been of interest for the information they contain on the short range nucleon-nucleon interaction and the role of meson exchange currents and relativistic effects. There are three form factors (charge G_C, magnetic G_M, and quadrupole G_Q) which can be determined from three experimentally measurable quantities:

$$A(Q^2) = G_C^2 + \frac{8}{9}\tau^2 G_Q^2 + \frac{2}{3}\tau G_M^2 \tag{3}$$

$$B(Q^2) = \frac{4}{3}\tau(1+\tau)G_M^2 \tag{4}$$

$$P(Q^2) = \frac{4\sqrt{2}}{3}\frac{\tau G_Q(G_C + \frac{\tau}{3}G_Q)}{(G_C^2 + \frac{8}{9}\tau^2 G_Q^2} \tag{5}$$

where $\tau = Q^2/4M_d^2$. The quantities $A(Q^2)$ and $B(Q^2)$ are measured using unpolarized electrons and deuterons at forward and backward angles respectively, while measurements of $P(Q^2)$ require the use of polarization.

The existing data[16] for $A(Q^2)$ are shown in Figure 6. Non-relativistic impulse approximation calculations tend to fall below the data, but can be brought into agreement using non-zero values for G_E^n, wave functions with strong high momentum components, or large relativistic corrections. Fits have also been made using parton models (see Ref. 15 for a review of calculations).

The structure function $B(Q^2)$ is a more sensitive test of models than $A(Q^2)$ since it is proportional to only one form factor (rather than three) as is predicted to have a diffraction minimum around $Q^2 = 2$ (GeV/c)^2. New data[17] have recently become available from an experiment at SLAC which detected electrons backscattered at 180° is coincidence with deuterons recoiling at 0°. The new data are shown as the solid circles in Figure 7 and do indeed show a minimum around $Q^2 = 2$ (GeV/c)^2. The non-relativistic impulse approximation using the Pairs wave function[18] has the minimum at too low a Q^2 (solid curve), but this is improved when isobar admixtures and isoscalar meson exchange currents are taken into account[19] (dashed curve) or when the wave function is treated relativistically[18] (dotted curve). Interestingly, the Skyrme model (expected to

work best at low Q^2) gives a result[20] indistinguishable from the dotted curve. Perhaps the most significant result is the strong disagreement with the smooth falloff of parton model predictions, an example[21] of which is shown as the dot-dashed curve.

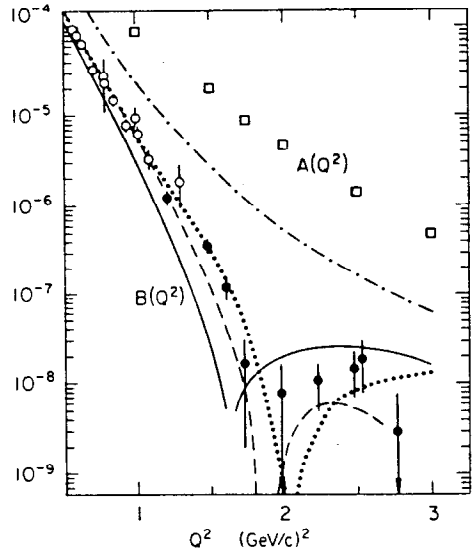

Fig. 7. Data for $B(Q^2)$ compared to various models (see text).

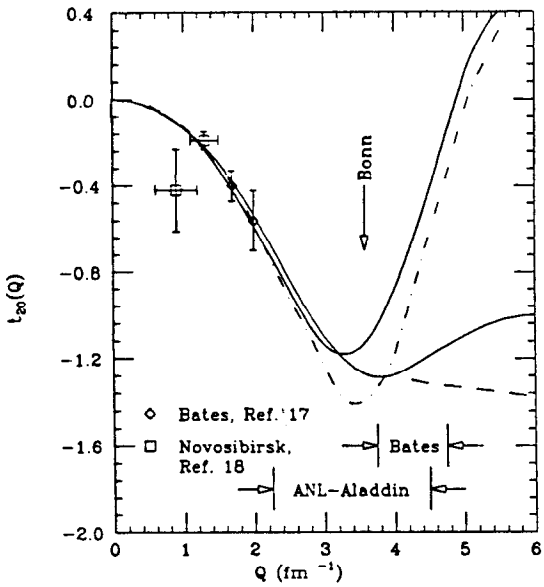

Fig. 8. Data[22] for t_{20} along with Q^2 ranges for future data. The dashed curve[23] is a QCD result, while the other curves are discussed in Ref. 24.

The data[22] for t_{20}, which is directly related to $P(Q^2)$) are shown in Figure 8. Data will soon be taken at Bates (see Figure for Q^2 range) which will go to high enough Q^2 to distinguish among various models. It will be especially interesting to see if QCD predictions[23] that t_{20} remain negative at large Q^2 are borne out. If the results support the traditional impulse approximation calculations (solid and dot-dashed curves in Figure 8), then increasingly tight constraints will be placed on models to simultaneously explain all the data for $A(Q^2)$, $B(Q^2)$, t_{20}, and the nucleon-nucleon scattering data.

DEUTERON THRESHOLD ELECTRODISINTIGRATION

The electrodisintigration of the deuteron near threshold has been shown to be one of the most sensitive reactions to non-nucleonic degrees of freedom (specifically isovector meson exchange currents).[26] The data[25] at backwards angles (where the M1 transition to the almost bound isospin triplet $^1S_0$ state dominates) averaged over excitation energies $E_{np} = 0$ to 3 Mev are shown in Figure 9. Impulse approximation calculations (not shown) fall far below the data at the higher Q^2, but the inclusion of MEC and isobar admixtures can bring calculations into reasonable agreement with the data.[26,27] Two areas of

uncertainty in the calculations are whether to use F_1^V or G_E^V in calculating the MEC, and in either case what is the size of G_E^n (see the four curves[26] shown in Figure 9). The somewhat more speculative hybrid quark cluster models[28] can find agreement with the data but predict a minimum in the cross section just where the data ends. This is contradiction to preliminary cross section data from experiment NE4 at SLAC[29] which continue to fall smoothly up to $Q^2 = 70$ fm^{-2}. The NE4 results have poor energy resolution ($\delta E_{np} = \pm 8$ MeV typically) but can still place significant limits on the cross section near threshold. A new experiment at Bates[30] has been approved to take data up to $Q^2 = 50$ fm^{-2} with good energy resolution. This new data will provide severe constraints on current models, complementary to those provided by measurements of $B(Q^2)$.

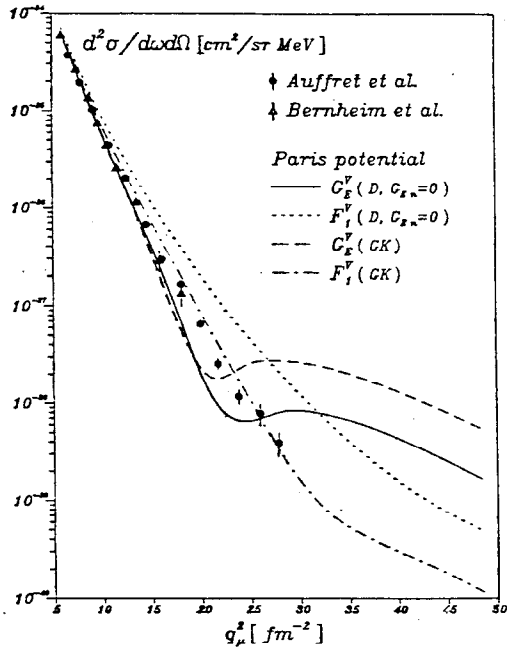

Fig. 9. Data[25] for $d(e,e')np$ averaged over $E_{np} = 0$ to 3 MeV compared to predictions[26] with different form factors.

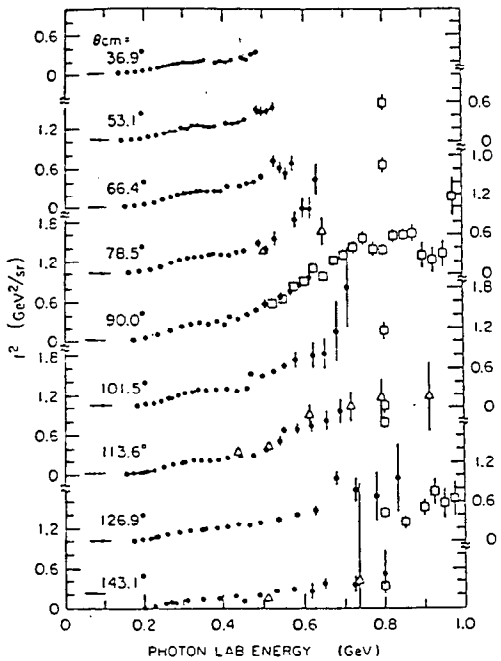

Fig. 10. Existing data[31] for photodisintigration of the deuteron with the s-dependence of QCD scaling[32] removed.

PHOTODISINTIGRATION OF THE DEUTERON

Another area where the importance of non-nucleonic degrees of freedom can be tested is in the photodisintigration of the deuteron. This is perhaps one of the simplest nuclear reactions, and has been studied in detail both experimentally[31] and theoretically at beam energies below 500 MeV, where the data is reasonably well described in terms of conventional meson-exchange theory.[33] Between 500 Mev and 1 Gev the small sample of data fall below the predictions. This has led

Brodsky and Hiller[32] to suggest that (at least around 90° in the c.m. system) the onset of dimensional scaling may have been reached. Dimensional scaling is based on lowest order perturbative QCD arguments and does very well is describing the energy dependence of meson photoproduction from the nucleon at energies above a few GeV. Dimensional scaling predicts that the reduced cross section

$$f^2(\theta_{CM}) = \frac{d\sigma}{d\Omega}\frac{\sqrt{s(s-M_d^2)}}{F_p(t_p)F_n(t_n)} \tag{6}$$

should be independent of s, the total energy in the c.m. system. The values for $f^2(\theta_{CM})$ for existing data[31] are plotted in Figure 10, where it can be seen that there is a hint of energy independence above 700 MeV. An experiment[34] is planned at SLAC in the near future to extend the data with reasonably small error bars up to 1.8 GeV. By the very nature of the kinematics involved, the new data will be very sensitive to the short range description of the nucleon-nucleon interaction, whether it be described in terms of extensions of the conventional model with additional N^* resonances, hybrid models including 6-quark clusters, bag models, or perturbative QCD.

QUASI-ELASTIC SCATTERING FROM DEUTERIUM

Quasi-elastic scattering from the lightest nucleus, the deuteron, is of particular interest since (below pion threshold) the final state is completely determined and relatively exact calculations can be made. As was discussed in a previous section, the area near the quasi-elastic peak can be used to determine the neutron form factor since the impulse approximation is believed to work well in this region. The region between threshold and the quasi-elastic peak is of particular interest because it is sensitive to the high-momentum components of the deuteron wave function. There exists a considerable amount of data at forward angles[35] which was compared[36] to the non-relativistic impulse approximation to estimate the deuteron wave function. Good agreement with the Paris wave function was found at low momenta ($P < 200$ MeV), but substantially higher values were found for $200 < P < 600$ MeV. Recent work[37] has shown that most of this discrepancy can be removed if the cross sections are compared to a calculation that takes into account final state interactions.

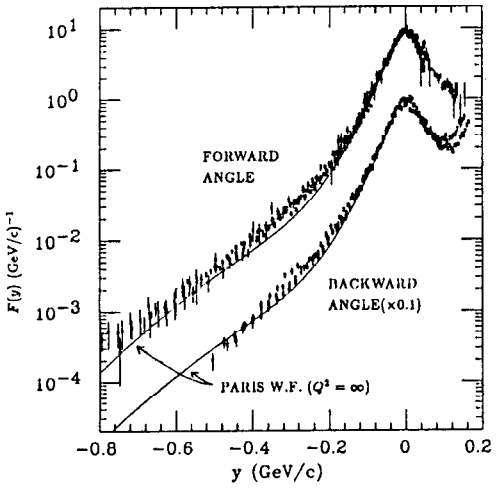

Fig. 11. $F(y)$ for forward angle data[35] (above) and preliminary backward angle data[29] (below).

There has recently become available cross section measurements at backward angles from Bates[38] at low Q^2, at Kharkov[39] for $0.5 < Q^2 < 1.0$ $(\mathrm{GeV/c})^2$, and at SLAC[29] for $1.0 < Q^2 < 2.75$ $(\mathrm{GeV/c})^2$. The new data allow comparisons of forward angle structure functions $W_2(Q^2, \nu)$ with backward angle structure functions $W_1(Q^2, \nu)$. The Kharkov data show that the ratio

$$R = \frac{\sigma_L}{\sigma_T} = \frac{W_2}{W_1}(1 + \frac{\nu^2}{Q^2}) - 1 \tag{7}$$

is small (< 0.3) near the quasi-elastic peak, as expected if scattering from spin-$\frac{1}{2}$ nucleons dominates, but becomes larger than 1.0 close to threshold. Calculations of R using the new SLAC data are presently underway. It will be interesting to see if this trend continues. Large values of R could indicate important contributions from scattering of spin-0 or spin-1 clusters.

Another common way of analyzing quasi-elastic data is in terms of y-scaling. First proposed by West[40] as a way of searching for universal single-particle momentum distributions in nuclei, it has been found to be remarkably successful in describing data over a large range of Q^2 and A. In the case of the deuteron a direct connection can be made between scaling functions and models, which can be shown to scale more or less well depending on the choice of variable and scaling function. For the definitions of y and $F(y)$ used in Ref. 36, both the forward angle[35] and preliminary backward angle SLAC data scale remarkably well, as shown in Figure 11. While the two data sets agree very well at the quasi-elastic peak, the backward angle $F(y)$ tends to be somewhat lower than the forward angle $F(y)$ for $y < 0.2$ GeV/c. Further analysis will be needed to interpret this difference.

THE EMC EFFECT AND R IN DEEP INELASTIC SCATTERING

The discovery of the difference in the structure functions $F_2(x)$ for iron and deuterium targets (the 'EMC effect') has sparked considerable activity in the theoretical study of deep inelastic scattering from nuclear targets. Models for the EMC effect (see Ref. 41 for a review) are built of ideas such as Q^2 rescaling, x-rescaling, binding effects, and contributions from clusters of pions, isobars, and so on. Some models[42] predict large differences for $R = \sigma_L/\sigma_T$ between iron and deuterium, while QCD models and others predict a negligible difference. An experiment to measure the difference in R was recently performed at SLAC. The preliminary results[43] are shown in Figure 12. It can be seen that the difference $R_{FE} - R_D$ is negligible over the x and Q^2 range studied, showing that there are no significant spin-0 constituents or higher twist effects in nuclei as compared to free nucleons. The new data also show that a nuclear dependence to R cannot be used to explain the difference between the lower Q^2, larger angle SLAC data and the higher Q^2, smaller angle CERN data for

σ^{FE}/σ^{D} at low x, as proposed by some authors.[44] It should be noted that the discrepancy at low x has been much reduced with the new CERN data (see Ref. 41 for a review).

The Q^2 dependence of R for hydrogen or deuterium is a sensitive probe of the transition region to perturbative QCD. At very large Q^2, R should be zero for scattering from spin-$\frac{1}{2}$ quarks, but at lower Q^2 target mass effects lead to a form of R which falls like powers of $1/Q^2$, while gluon processes lead to a form which falls like $1/\ln(Q^2/\Lambda^2)$ (see for example Ref. 45). The preliminary data from SLAC E140 for R_D at $x = .2$ (and a high Q^2 data point from CDHS for iron) are shown as a function of Q^2 in Figure 13. Good agreement is found with the upper curve, which includes both gluon contributions and target mass corrections. Similar agreement is found at higher values of x. The errors on the SLAC R_D values will shrink when the analysis of radiative corrections is completed.

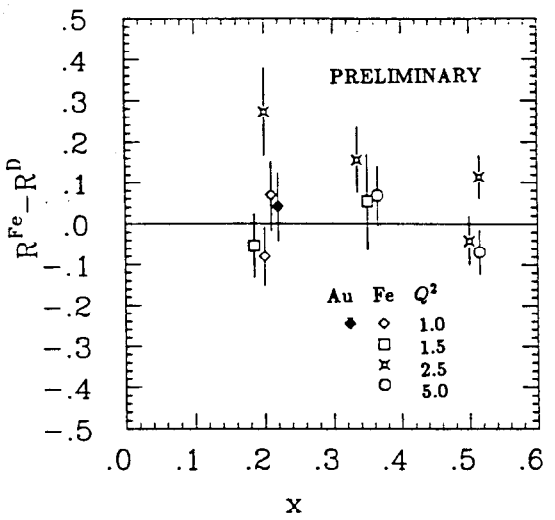

Fig. 12. Preliminary values of $R_{FE} - R_D$ as a function of x for various Q^2 values from SLAC E140 experiment.[43]

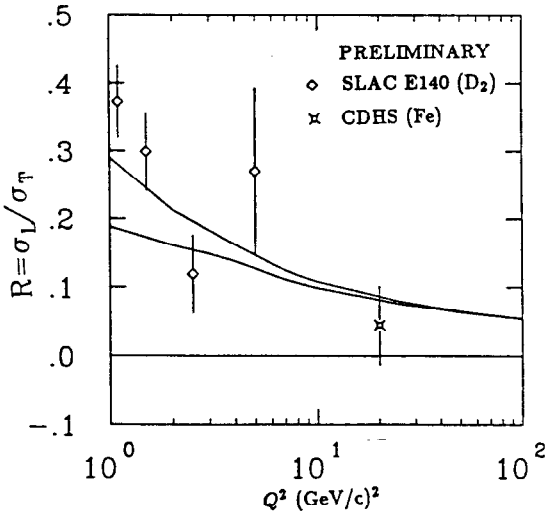

Fig. 13. R vrs Q^2 at $x = 0.2$. The lower curve is a perturbative QCD calculation including gluon contributions, while the upper curve also includes target mass contributions.

CONCLUSIONS

The examples cited in this paper show that experiments measuring the electromagnetic properties of few body systems are pushing towards ever higher energies and precision. These data provide stringent tests of our understanding of short range properties and non-nucleonic degrees of freedom. Theoretical approaches using PQCD, bag models, relativistic nucleon and meson models, the Skyrme model, and so-called hybrid models are making progress in their

ability to quantitatively understand the results obtained so far and make predictions that will be tested by future experiments. The availability of 4 to 6 GeV high current, high duty factor polarized electron beams at CEBAF, in combination with polarized targets or polarimeters, will open a new frontier in making precision measurements of quantities such as the neutron form factor, the transition form factors of the nucleon resonances, the deuteron t_{20} at high Q^2, and the ΛN interaction. Experiments which require higher energy, such as hadronization in deep inelastic scattering or measurements of the deep inelastic spin structure functions of the nucleon are being studied for feasibility using internal targets at the PEP storage ring. At very high energies, measurements in the deep inelastic region using muons continue to be made at Fermilab[46] and CERN.[47] Pushing the frontiers of the few-body electromagnetic problem will continue to keep us busy for many years to come.

REFERENCES

1. R. G. Arnold, AIP Conference Proc. 150, p.83 (1986); R. R. Whitney, 'Electromagnetic Interactions with Few-Body Systems', XI Int. Conf. Part. Nuclei, Kyoto, Japan, April 1987; B. Frois and C. Papanicolas, 'Electron Scattering and Nuclear Structure', U. Illinois preprint P/87/7/118.
2. G. Höhler et al., Nucl. Phys. B114, 505 (1976); S. Blatnk, N. Zovko, Acta Phys. Austriaca 39, 62 (1974); F. Iachello, A. Jackson, A. Lande, Phys. Lett. 43B, 191 (1973).
3. R. Arnold et al., Phys. Rev. Lett. 57, 174 (1986).
4. S. Brodsky, G. Lepage, Phys. Rev. D22, 2157 (1980).
5. V. L. Chernyak, I. R. Zhitnitsky, Nucl. Phys. B246, 52 (1984): V. L. Chernyak, I. R. Zhitnitsky, Phys. Rep. 112, 1973 (1984).
6. M. Gari, W. Krumpelmann, Z. Phys. A322, 689 (1986).
7. M. Anselmino, P. Kroll, B. Pire, WU B 87-2, February 1987.
8. R. Walker et al., SLAC experiment E140, to be published.
9. SLAC experiment NE11, P. Bosted spokesman.
10. S. Rock et al., Phys. Rev. Lett. 49, 1139 (1982); R. J. Budnitz et al., Phys. Rev. 173, 1357 (1968); W. Albrecht et al., Phys. Rev. 26B, 642 (1968).
11. J. G. Körner, M. Kuroda, Phys. Rev. D16, 2165 (1977).
12. R. Arnold et al., Phys. Rev. C21, 1426 (1980).
13. Z. Meziani et al., Phys. Rev. Lett. 54, 1233 (1985) and references therein.
14. O. Benhar et al., INFN-ISS-87/1 (1987).

15. V. M. Muzafarov et al., Fiz. Elem. Chastits At Yadra 14, 1112 (1983) [Sov. J. Part. Nucl. 14, 467 (1983)].

16. R. G. Arnold et al., Phys. Rev. Lett. 35, 776 (1975).

17. R. G. Arnold et al., Phys. Rev. Lett. 58, 1723 (1987).

18. R. S. Bhalero and S. A. Gurvitz, Phys. Rev. C24, 2273 (1981).

19. E. Lomon et al., Proc. IUPAP Int. Nucl. Phys. Conf., Vol. I, p. 478.

20. E. M. Nyman and D. O. Riska, Phys. Rev. Lett. 57, 3007 (1986).

21. M. Chemtob and S. Furui, Nucl. Phys. A454, 548 (1986).

22. M. E. Schultz et al., Phys. Rev. Lett. 52, 597 (1984); Y. F. Dmitriev et al., Phys. Lett. 157B, 143 (1985).

23. C. E. Carlson and F. Gross, Phys. Rev. Lett. 53, 127 (1984).

24. W. Turchinetz, Proc. Eur. Work. Few-Body Phys., Rome, 1986, p. 326.

25. S. Auffret et al., Phys. Rev. Lett. 55, 1362 (1985); M. Berheim et al., Phys. Rev. Lett. 46, 402 (1981).

26. H. Arenhovel, Mainz Preprint MKPH-T-87-4.

27. J. Mathiot, Nucl. Phys. A412, 210 (1984).

28. T.-S. Cheng, L. S. Kisslinger, Nucl. Phys. A457, 602 (1986): Y. Yamauchi et al., Nucl. Phys. A443, 628 (1985).

29. SLAC Experiment NE4, G. Petratos and P. Bosted, private communication.

30. R. Miskamen and G. Peterson, spokesmen.

31. J. Arends et al., Nucl. Phys. A412, 509 (1984) and references therein.

32. S. J. Brodsky and J. R. Miller, Phys. Rev. C28, 475 (1983).

33. J. M. Laget, Nucl. Phys. A312, 265 (1978).

34. SLAC Experiment NE8, R. Holt spokesman.

35. W. P. Schultz et al., Phys. Rev. Lett., 38, 259 (1977); S. E. Rock et al., Phys. Rev. Lett., 49, 1139 (1982).

36. P. E. Bosted et al., Phys. Rev. Lett., 49, 1380 (1982).

37. C. degli Atti et al., Nucl. Phys. A463, 127 (1987).

38. B. Parker et al., Phys. Rev. C 34, 2354 (1986): A. Bernstein et al., to be published.

39. Yu. I. Titov, Kharkov Preprint KPTI 87-38.

40. G. B. West, Phys. Rep. 18C, 263 (1975).

41. E. L. Berger and F. Coster, ANL-HEP-PR-87-13 (1987).

42. B.-Q. Ma and Ji Sun, Print-86-1217, Beijing U. (1986).

43. S. Dasu et al., UR-991 and UR-998 (Rochester 1987).

44. I. A. Savin and G. I. Smirnov, Phys. Lett. 145B, 438 (1984).

45. G. Altarelli and G. Martinelli, Phys. Lett. 28B, 89 (1978).

46. Fermilab experiment E665, PHY-4622-ME-85.

47. D. Allasia et al., the New Muon Collaboration, CERN Proposal SPSC/P210.